Journal of
Materials Chemistry A

Accepted Manuscript

This article can be cited before page numbers have been issued, to do this please use: J. H. Park, F. Raza, S. Jeon, D. Yim, H. Kim, T. W. Kang and J. Kim, *J. Mater. Chem. A*, 2016, DOI: 10.1039/C6TA04278C.

ROYAL SOCIETY OF CHEMISTRY

www.rsc.org/materialsA

View Article Online
DOI: 10.1039/C6TA04278C

Journal of Materials Chemistry A

PAPER

Oxygen-mediated Formation of MoS_x-doped Hollow Carbon Dots for Visible Light-driven Photocatalysis†

Received 00th January 20xx,
Accepted 00th January 20xx

DOI: 10.1039/x0xx00000x

www.rsc.org/

Jung Hyun Park, Faizan Raza, Su-Ji Jeon, DaBin Yim, Hye-In Kim, Tae-Woog Kang, and Jong-Ho Kim*

It is of great interest to modulate the photocatalytic activity of nanomaterials by varying their composition at atomic scale and their nanostructure. Herein, we demonstrated a bottom-up approach for synthesis of MoS_x-doped hollow carbon dots ($_{MoS}$HCDs) as a photocatalyst for the visible light-driven aerobic oxidative coupling of amines. The molecular oxygen-assisted solvothermal reaction of a MoS_2 nanosheets/*N*-methyl-2-pyrrolidone dispersion provided $_{MoS}$HCDs with a unique hollow interior of 6-7 nm as well as with doping of a large portion of pyridinic N atoms and MoS_x. As compared to typical carbon dots not bearing hollow structure, as-prepared $_{MoS}$HCDs exhibited more excellent photocatalytic activity in the oxidative coupling reactions of various amines under visible light irradiation at 25 °C. Mechanistic investigations suggested that doping with pyridinic N atoms and MoS_x was responsible for the significantly improved photocatalytic activity of $_{MoS}$HCDs in the photocatalysis. The reaction mechanism of the oxidative coupling reactions of amines that were effectively promoted by $_{MoS}$HCDs under visible light irradiation was also fully examined.

Introduction

Carbon nanodots, such as carbon dots (CDs) and graphene quantum dots (GQDs), have received tremendous attention in diverse research fields due to their superior properties compared to conventional semiconductor quantum dots.[1, 2] The physicochemical properties of CDs and GQDs can be tuned effectively by heteroatom-doping[3-5] or surface passivation with organic and inorganic components.[6-9] In this regard, numerous efforts have been devoted to improving their quantum yield (QY) *via* doping and surface passivation, and then mostly to demonstrating their potential as an alternative to organic fluorescent dyes in bioimaging.[1] Conversely, only a few studies have demonstrated how heteroatom doping and surface passivation can alter the catalytic activity of carbon nanodots.[10-12] In particular, investigations regarding how doping and functionalization can modulate the photocatalytic activity of carbon nanodots in useful organic transformations driven by visible light are lacking, despite the fact that their activity could be significantly altered. Therefore, the precise design of carbon nanodots with high photocatalytic activity for the visible light-driven transformation of organic compounds is still needed.

Imines are important organic compounds for the synthesis of pharmaceuticals, agrochemicals, dyes and fine chemicals.[13] Aerobic oxidation of amino compounds is an effective method for producing various imines, which has been conducted in the presence of metal catalysts under generally harsh conditions.[14] Recently, several environmentally-benign approaches utilizing visible light as a driving force were reported for the aerobic oxidation of various amines into corresponding imines.[15-19] These methods showed promise in the photocatalyzed production of imines with high yields. However, to effectively promote the aerobic oxidation of amines under visible light irradiation, precisely designed photocatalysts are needed. Well-defined CDs are potentially effective candidates for photocatalyzing the aerobic oxidative coupling of amines under visible light irradiation since they were found to strongly absorb visible light and emit intense fluorescence with high quantum yields in the visible range, but, there have been no reports to date.[20-22] In particular, modulating the photocatalytic activity of CDs *via* doping with MoS_x in this reaction is important since MoS_x can promote O_2 activation, an essential step in the aerobic oxidative coupling reaction of amines.[23]

Herein, we report a novel approach for the bottom-up synthesis of MoS_x-doped hollow CDs ($_{MoS}$HCDs) that can promote the visible light-driven oxidative coupling reaction of various amines at room temperature (rt). $_{MoS}$HCDs were readily synthesized *via* the molecular oxygen-assisted solvothermal reaction of a MoS_2 nanosheets/*N*-methyl-2-pyrrolidone (NMP) dispersion. After full characterization of the $_{MoS}$HCDs properties, their photocatalytic activity in the aerobic oxidative coupling reaction of amines under visible light irradiation was investigated, and then was compared to that of typical carbon dots without hollow structure. Additionally, in this study we

Department of Chemical Engineering, Hanyang University, Ansan 426-791, Republic of Korea
* E-mail: kjh75@hanyang.ac.kr
† Electronic Supplementary Information (ESI) available: Materials, experimental procedures, and additional supporting data. See DOI: 10.1039/x0xx00000x

View Article Online
DOI: 10.1039/C6TA04278C

demonstrated the mechanism responsible for the outstanding photocatalytic activity of $_{MoS}$HCDs in the aerobic oxidative coupling of amines as well as the mechanism for this photocatalysis.

Experimental

Materials

Molybdenum disulfide (MoS_2), benzylamine, 4-methylbenzylamine, 4-methoxybenzylamine, piperonylamine, 4-chlorobenzylamine, 2-picolyamine, 2-thiophenemethylamine, 1-phenylethylamine, dibenzylamine, benzoquinone and coumarin 153 were purchased from Sigma-Aldrich (USA). 4-tert-Butylbenzylamine, 2,4-dichlorobenzylamine, and heptylamine were purchased from Tokyo Chemical Industry (Japan). 2-Methylbenzylamine, 4-fluorobenzylamine, tetra-n-butylammonium perchlorate, and Ag wire were purchased from Alfa Aesar (USA) and used without purification. Acetonitrile, *N*-methyl-2-pyrrolidone, ethanol and toluene were purchased from Dae-Jung Chemicals (Korea). Dialysis membrane (spectra/Por®, MWCO: 1,000) and alumina membrane filter (Anodisc 47, 20nm) were provided by Spectrum® Laboratories (USA) and Whatman™ (USA), respectively.

Preparation of MoS_x-doped Hollow Carbon Dots ($_{MoS}$HCDs)

To synthesize $_{MoS}$HCDs, bulk MoS_2 (500mg) was added into *N*-methyl-2-pyrrolidone (NMP, 200ml), and the resulting solution was sonicated using a probe sonicator (140 W) for 3 h in an ice bath. The mixture was then centrifuged at 500 g-force for 60 min, and a 75 % portion of supernatant was collected to obtain an exfoliated MoS_2 nanosheets/NMP dispersion. Then, a 20 ml portion of MoS_2 nanosheets/NMP dispersion in a two-necked round bottom flask was heated up with stirring for 3 h at 140 °C under O_2 or Ar atmosphere. After cooling down to room temperature, the reaction mixture was filtered with alumina membrane filter (20 nm pore), and the filtrate was concentrated under vacuum at 100°C for 6 h. The concentrated solution was diluted with 20 mL of water, which was then purified *via* dialysis with a membrane tube (MWCO 1,000) for 1 day. The product, $_{MoS}$HCDs, were lyophilized at - 40 °C overnight.

Aerobic oxidative coupling reaction of amines under visible light irradiation

A photocatalyst (2 mg) was dispersed in 10 ml of an acetonitrile and NMP mixture (7 : 3) in a glass vial with an open top septa cap *via* light sonication. A 0.1 mmol portion of amine and 5 μl of toluene as an internal standard were added into the catalyst solution. Then, the mixture was stirred in the presence of molecular O_2 under visible light irradiation using two 60 W cool white LED lamps (LED SIGN ART, Korean) at room temperature. The reaction was monitored by gas chromatography as a function of time. After a certain period of time, the reaction yields were calculated. For the heterocoupling reaction of amines, a 0.1 mmol portion of benzylamine and a 0.3 mmol portion of heptylamine were added to the reaction mixture.

The reaction yield was calculated using pre-synthesized imine products from amine and aldehyde.[24, 25] To synthesize imine product, 5 mmol of amine, 5 mmol of aldehyde and 0.5 mg of $MgSO_4$ were added to 5 ml of CH_2Cl_2. The reaction mixture was stirred for 5 h at room temperature and then $MgSO_4$ was removed by filtering. The solvent was vaporized using rotary evaporator, and unreacted amine and aldehyde were vaporized under vacuum at 60 °C. The calibration curve was obtained using toluene as an internal standard and each imine product to calculate the yield of the oxidative coupling reaction of amines. Except *N*-(4-(tert-butyl)benzyl)-1-(4-(tert-butyl)phenyl) methanimine, all other products exhibited a same slope of calibration curves.

To study the effect of light power intensity and wavelength on the catalytic activity of $_{MoS}$HCDs, a xenon lamp (300 W, Newport, USA) with a 400 nm long wave pass cut-on filter and a liquid filter was utilized. For the study of power intensity effect on the catalytic activity, the light intensity was varied from 14, 70, to 210 mW/cm² by adjusting the distance between the reactor and the lamp. For study of light wavelength effect on the catalytic activity, a 590 nm long wave pass cut-on filter was equipped into the xenon lamp with a 210 mW/cm² of power.

Results and Discussion

Bottom-up synthesis of $_{MoS}$HCDs

To synthesize $_{MoS}$HCDs, a MoS_2 nanosheets/NMP dispersion was obtained *via* a simple liquid exfoliation of bulk MoS_2 in

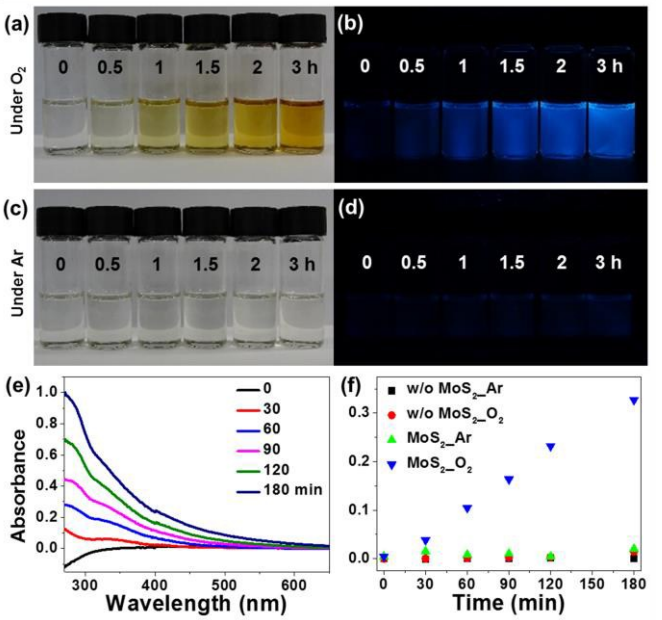

Figure 1. Real-time monitoring of $_{MoS}$HCDs formation. (a) Optical and (b) fluorescence images of a MoS_2 nanosheets/NMP dispersion as a function of reaction time at 140 °C under O_2. (c) Optical and (d) fluorescence images of a MoS_2 nanosheets/NMP dispersion under Ar gas. (e) Absorption spectra of $_{MoS}$HCDs, and (f) Absorbance of various solutions at 372 nm as a function of reaction time at 140 °C. (w/o: without)

View Article Online
DOI: 10.1039/C6TA04278C

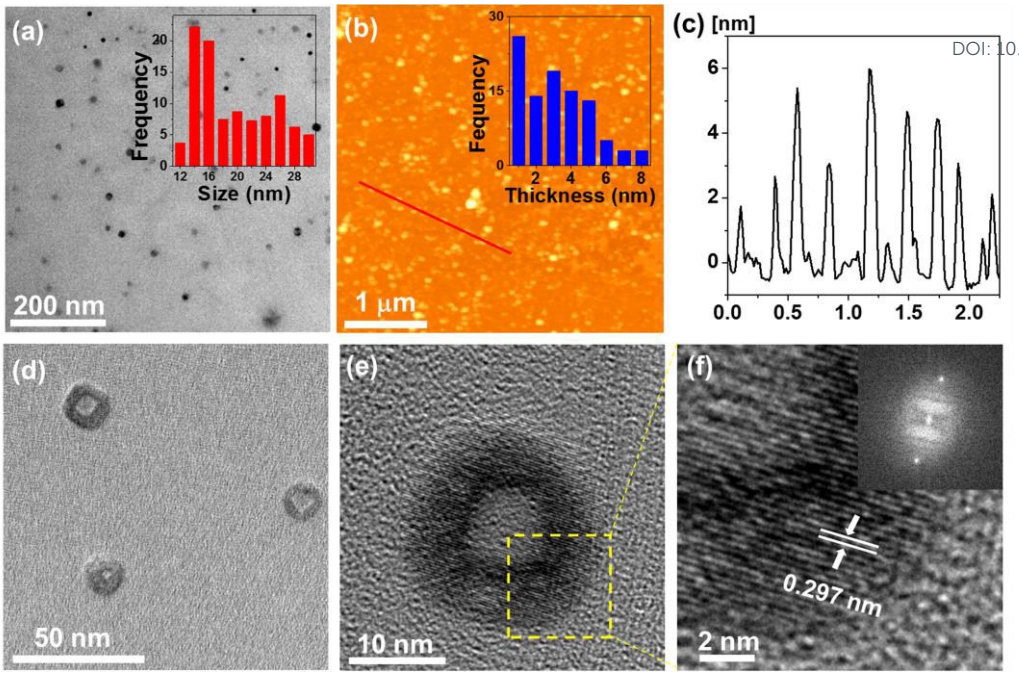

Figure 2. Characterization of $_{MoS}$HCDs. (a) TEM image of $_{MoS}$HCDs (Inset: size distribution). (b) AFM image of $_{MoS}$HCDs (Inset: thickness distribution), and (c) height profile for a red line in (b). (d) HR-TEM and (e) magnified images of $_{MoS}$HCDs. (f) Lattice structure of $_{MoS}$HCDs (Inset: FFT pattern).

NMP, as previously reported.[26] Then, the MoS_2/NMP solution was heated at 140 °C under O_2 atmosphere. As shown in Fig. 1a, the solution color turned very quickly into dark yellow, which exhibited very strong fluorescence under a 365 nm ultraviolet (UV) lamp (Fig. 1b). However, under an Ar atmosphere, no change of the solution color was observed, even 3 h after heating (Fig. 1c) and no fluorescence emission appeared (Fig. 1d). This result indicates that molecular oxygen plays a crucial role in the formation of $_{MoS}$HCDs. For comparison, pure NMP not containing MoS_2 nanosheets was also heated at 140 °C for 3 h under O_2. As shown in Fig. S1a, the solution color rarely changed until 2 h, but turned light yellow after 3 h. This solution also showed weak fluorescence (Fig. S1b), but the obtained fluorescent nanomaterials (denoted NMP-CDs) were typical CDs without hollow structure, as discussed later. Pure NMP did not change color in 3 h after heating under an Ar atmosphere (Figs. S1c and S1d). These control experiments indicated that MoS_2 nanosheets affect the structure of $_{MoS}$HCDs as well as accelerate their formation. The formation kinetics of $_{MoS}$HCDs was quantitatively monitored by measuring their absorption characteristics, which exhibited strong absorption in the visible range as well as in the UV region (Fig. 1e). The absorbance of $_{MoS}$HCDs at 372 nm was plotted as a function of the heating time (Fig. 1f), showing the formation of $_{MoS}$HCDs was accelerated only in the presence of both O_2 and MoS_2 nanosheets. However, the absorbance of pure NMP heated at 140 °C for 3 h, in which a few NMP-CDs formed, did not increase as much as $_{MoS}$HCDs, indicating that the formation of NMP-CDs did not effectively occur (w/o MoS_2_O_2 in Fig. 1f and Fig. S2).

Characterization of $_{MoS}$HCDs

Next, we analyzed the structure of $_{MoS}$HCDs using

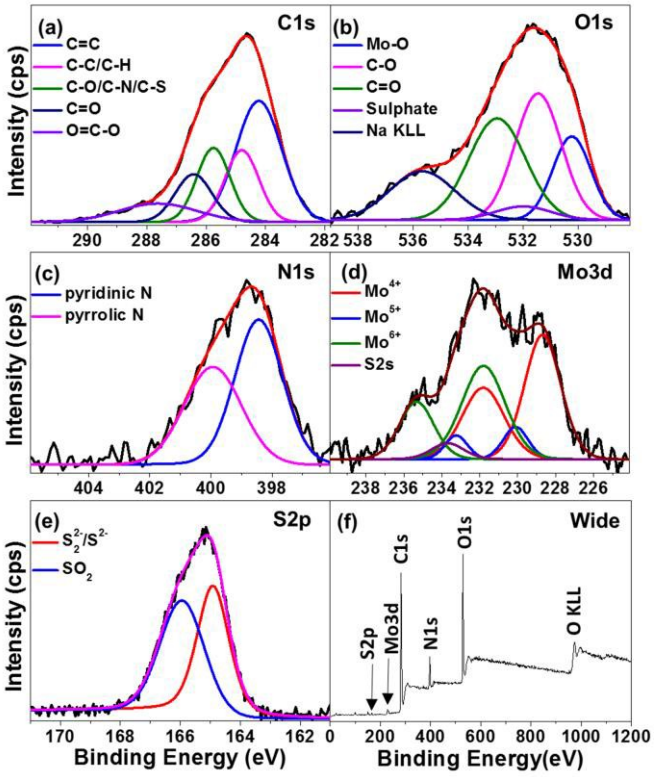

Figure 3. XPS analysis of $_{MoS}$HCDs. XPS spectra for (a) C1s, (b) O1s, (c) N1s, (d) Mo 3d, (e) S2p and (f) wide scan.

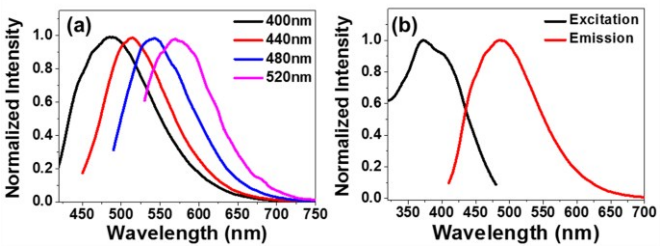

Figure 4. Optical property of $_{MoS}$HCDs. (a) Excitation-dependent emission of $_{MoS}$HCDs, (b) photoluminescence excitation (PLE) spectrum at an emission of 500 nm and photoluminescence (PL) spectrum of $_{MoS}$HCDs at an excitation of 400 nm.

transmission electron microscopy (TEM) and atomic force microscopy (AFM), as shown in Figure 2. The structures were quasi-spherical in shape with an average size of 22.13 nm, which is larger than most of the CDs previously reported (Fig. 2a). In addition, $_{MoS}$HCDs were 3.43 nm in topographical height (Figs. 2b and 2c). They had a bright center as shown in Fig. 2d, indicating a hollow interior. Figure 2e more clearly shows the 6.5-nm hollow interior of $_{MoS}$HCDs and a 7.5-nm carbon shell. In addition, the carbon shell had a well-defined crystal structure with a lattice spacing of 0.297 nm (Fig. 2f), consistent with the basal spacing of graphite. The X-ray diffraction (XRD) spectrum of $_{MoS}$HCDs reveals that the interlayer spacing of $_{MoS}$HCDs was 0.37 nm (Fig. S4), which is very close to that of graphite.[27] We also analyzed NMP-CDs obtained by heating pure NMP under an O_2 atmosphere. Interestingly, NMP-CDs had no hollow interior (Figs. S3a and S3b) and were much smaller in size (ca. 5 nm) with a lattice spacing (0.21 nm) smaller than $_{MoS}$HCDs. These results indicate the presence of MoS_2 nanosheets during a formation reaction led to hollow-structured CDs.

The chemical composition of $_{MoS}$HCDs was analyzed using X-ray photoelectron spectroscopy (XPS) and was compared with NMP-CDs. As shown in Figure 3, $_{MoS}$HCDs were mainly composed of C, N, O, S and Mo, while NMP-CDs consisted of C, N and O atoms (Figs. S3c-S3f). As shown in the C1s spectrum of $_{MoS}$HCDs (Fig. 3a), the peaks for C=C and C-C bonds appeared at 284.8 and 284.2 eV, respectively. In addition, the peaks observed at 285.8, 286.4 and 287.63 eV can be assigned to C-S/C-N/C-O, C=O and O-C=O bonds. The Mo-O chemical bond

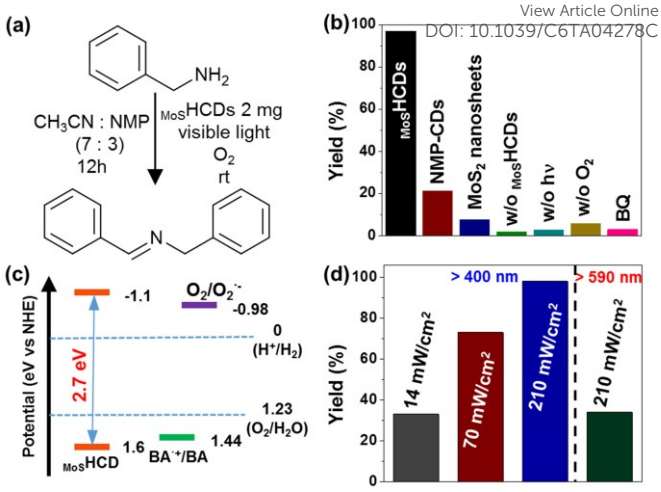

Figure 5. Visible light-driven aerobic oxidative coupling of BA catalyzed by $_{MoS}$HCDs. (a) Reaction scheme, (b) Product yields at various reaction conditions and (c) Potential energy diagram for $_{MoS}$HCDs, O_2 and BA. (d) Light power and wavelength effect on the photocatalytic activity of $_{MoS}$HCDs in the oxidative coupling reaction of BA.

was also observed at 530.2 eV (Fig. 3b). Notably, $_{MoS}$HCDs had a larger portion of pyridinic N (398.4 eV) rather than pyrrolic N (399.9 eV), as shown in Figure 3c. However, NMP-CDs had mostly pyrrolic N (Fig. S3e). This variation in nitrogen species alters their photocatalytic activity in the aerobic oxidative coupling of amines. The specific peaks of Mo^{4+} (228.7, 231.8 eV), Mo^{5+} (230.3, 233.41 eV) and Mo^{6+} (232.0 and 235.3 eV) were clearly observed (Fig. 3d), indicating that the $_{MoS}$HCDs were successfully doped with Mo atoms. According to the result of inductively coupled plasma atomic emission spectroscopy (ICP-AES), 0.15 wt % of Mo was included in the MoSHCDs. In the S2p spectrum of $_{MoS}$HCDs (Fig. 3e), bridging S_2^{2-} and apical S^{2-} appeared at 164.9 eV.[28] The additional peak at 165.9 eV was assigned to SO_2.[29] The XPS analysis reveals that the atomic ratio between molybdenum and sulfur atoms was 1:1.17, indicating that molybdenum sulfide species were embedded into the CDs. The several oxidation states of molybdenum sulfide could be generated through the oxidation of dissolved MoS_2 by NMP radicals and oxygen during solvothermal reactions.

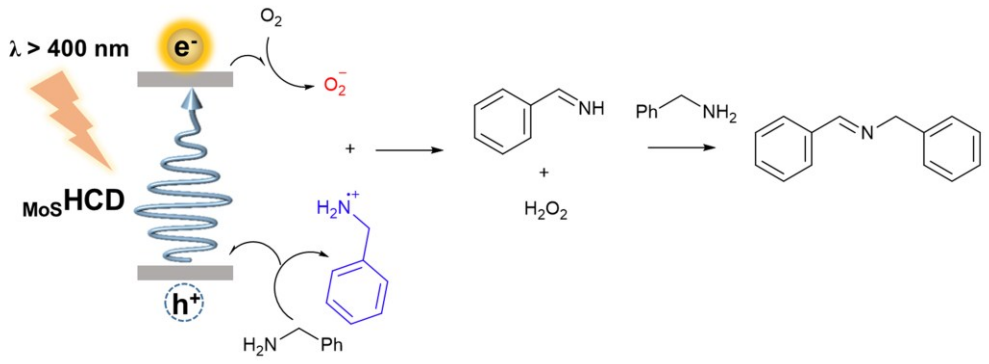

Scheme 1. Reaction mechanism for the aerobic oxidative coupling of amines photocatalyzed by $_{MoS}$HCDs.

View Article Online
DOI: 10.1039/C6TA04278C

Table 1. Oxidative coupling reactions of various amines photocatalyzed by $_{MoS}$HCDs[a]

Entry	Substrate	Product	Time	Yield (%)[b]
1	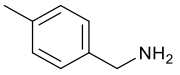	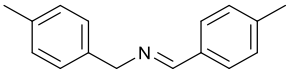	12	95
2	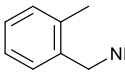	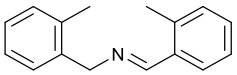	12	95
3	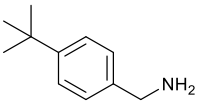	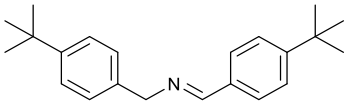	12	94
4	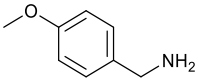	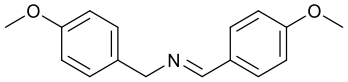	12	98
5	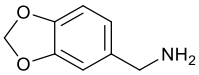	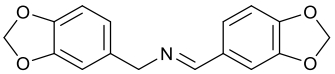	12 (24)	64 (97)[c]
6	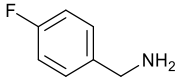	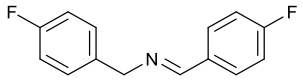	12	88
7	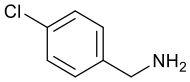	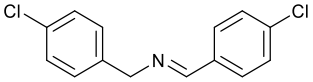	12	89
8	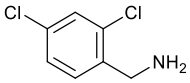	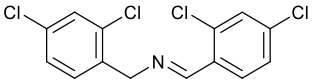	12 (24)	60 (87)[c]
9	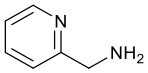	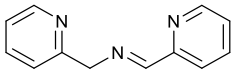	12 (24)	50 (56)[c]
10	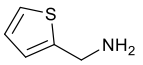	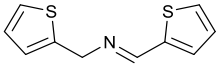	12	86
11	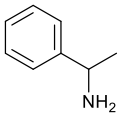	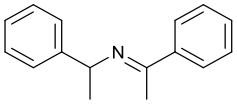	12 (24)	23 (11)[c]
12	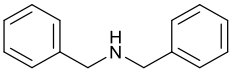	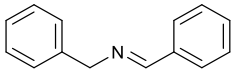	12	94
13	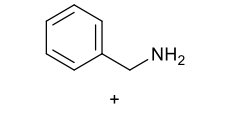	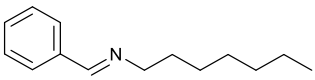	12	67[d]

[a]Amine (0.1 mmol), $_{MoS}$HCDs (2 mg), acetonitrile:NMP (7:3), cool white LED lamp (60W). [b]Yield calculated by gas chromatography using toluene as an internal standard. [c]Yield for 24 h. [d]Benzylamine (0.1 mmol) and heptylamine (0.3 mmol) were used for the reaction.

To investigate the mechanism responsible for the formation of $_{MoS}$HCDs, we analyzed the MoS_2 nanosheets/NMP reaction mixture at the middle of the reaction using nuclear magnetic resonance (NMR) spectroscopy. As shown in Figure S6, the characteristic peaks for the formation of several oxidized products of NMP such as *N*-methylsuccinimide, 4-(methylamino)-4-oxobutanoic acid and 2-pyrrolidone were observed. Reportedly, NMP can be oxidized by molecular O_2 at high temperatures to produce these oxidized products.[30, 31] During the course of NMP oxidation, H_2O is also produced as a byproduct. This oxidation process is significantly accelerated by MoS_2 nanosheets, resulting in the rapid production of polymers bearing five- and six-membered heterocycles as well as abundant H_2O in the reaction mixture. Then, these polymers bearing five- and six-membered heterocycles are carbonized. We speculated that the H_2O molecules could produce nano-bubbles at elevated temperatures higher than their boiling point during polymerization/carbonization, which might create a hollow interior in $_{MoS}$HCDs.

We investigated the fluorescent property of $_{MoS}$HCDs, which showed excitation wavelength-dependent fluorescence emission (Fig. 4a). As previously reported,[2, 9] this fluorescence shift can be attributed to the presence of different surface states and inhomogeneity in the $_{MoS}$HCD size. The $_{MoS}$HCDs exhibited excitation and emission maxima at 372 and 487 nm, respectively (Fig. 4b) and a quantum yield of 13%. NMP-CDs showed similar fluorescence emission, but exhibited much weaker absorption in visible region (Fig. S5).

Visible-light driven oxidative coupling reaction of amines

Then, we evaluated the photocatalytic activity of $_{MoS}$HCDs in the oxidative coupling reaction of amines under visible light irradiation (Fig. 5a). As a model substance, benzylamine (BA, 10.7 mg) was used to yield a corresponding product, *N*-benzylidenebenzylamine (NBBA), catalyzed by $_{MoS}$HCDs (2 mg) under a cool white LED lamp (60 W, > 400 nm). The reaction was conducted at rt under O_2 atmosphere. Figure 5b shows that BA was converted into NBBA with high yield (97%), indicating that $_{MoS}$HCDs are very active photocatalysts in this reaction. However, NMP-CDs (2 mg) showed much weaker photocatalytic activity in the oxidative coupling of BA (21% yield). This comparison suggests that doping and chemical composition can significantly alter the photocatalytic activity of CDs in the reaction. The much higher photoactivity of $_{MoS}$HCDs in the aerobic oxidation of amines is due to the greater portion of pyridinic nitrogen in $_{MoS}$HCDs than NMP-CDs that have mostly pyrrolic nitrogen. Since pyridinic nitrogen is more basic than pyrrolic nitrogen, the aerobic oxidation of amines can be enhanced by $_{MoS}$HCDs. According to the simulation results, pyridinic nitrogen was found a more active species for oxygen reduction reactions.[32] Another important reason for the outstanding photocatalytic activity of $_{MoS}$HCDs is MoS_x doping, which facilitates O_2 activation, a crucial step in this reaction.[23]

To understand the reaction mechanism responsible for the aerobic oxidative coupling of amines photocatalyzed by $_{MoS}$HCDs, further control experiments were performed. As shown in Figure 5b, BA was rarely converted into NBBA in the absence of $_{MoS}$HCDs. In addition, the oxidative coupling of BA did not occur without light irradiation, even in the presence of $_{MoS}$HCDs. After removing O_2 by purging with Ar gas, the product yield dramatically decreased to 5.6% in the presence of $_{MoS}$HCDs under light irradiation. This small amount of product might be produced by coupling of benzylimine, which could be generated by dehydrogenation of benzylamine, with other benzylamine as reported in other literatures.[15, 33] These results clearly indicate that the oxidative coupling of BA into NBBA was photocatalyzed by $_{MoS}$HCDs under an O_2 atmosphere. According to a previous report,[34] O_2 is converted into superoxide by obtaining an excited electron from a photocatalyst, and then this superoxide reacts with an oxidized amine to produce an imine intermediate. To confirm this in the $_{MoS}$HCDs-catalyzed oxidative coupling of amine, benzoquinone (BQ), a superoxide scavenger, was added into the reaction mixture. As shown in Figure 5b, the production yield of NBBA significantly decreased to 2.9%. This result indicates that the O_2 activation through an electron transfer from $_{MoS}$HCDs is a crucial step in the aerobic oxidative coupling reactions. The plausibility for electron transfer from $_{MoS}$HCDs to O_2 was confirmed by measuring the edge positions of $_{MoS}$HCDs using cyclic voltammetry (Fig. S7). As shown in the energy diagram (Fig. 5c), the potential of the conduction band of $_{MoS}$HCDs was higher than that required for the conversion of O_2 into superoxide. Additionally, the potential of the valence band of $_{MoS}$HCDs was lower than for the oxidation of BA, allowing the electron transfer from BA to $_{MoS}$HCDs. This electron transfer was indirectly confirmed by measuring the fluorescence quenching of $_{MoS}$HCDs by BA. As shown in Figure S8, the fluorescence of $_{MoS}$HCDs was gradually diminished with increased concentration of BA, indicating the electron transfer from BA to $_{MoS}$HCDs. This reductive fluorescence quenching was also observed in other fluorophores.[35-37]

Based on the experimental results, we proposed the reaction mechanism for the aerobic oxidative coupling of amines photocatalyzed by $_{MoS}$HCDs (Scheme 1). After $_{MoS}$HCDs absorb visible light, the excited electron is transferred to O_2 to produce superoxide and the electron of BA is transferred to $_{MoS}$HCDs to yield the oxidized BA. These two intermediates then react to produce benzylimine along with H_2O_2 as a byproduct, which was confirmed by NMR (Fig. S9). Finally, benzylimine reacts with another BA to produce the product NBBA.

We investigated the effect of light power density and wavelength on the photocatalytic activity of $_{MoS}$HCDs during the reaction of BA (Fig. 5d). As the light power density increased from 14, 70, and to 210 mW/cm^2 (> 400 nm), the reaction yields gradually increased from 33 to 98%. As expected, the higher density of photons can create the more number of excited electrons in the conduction band of $_{MoS}$HCDs for triggering the reaction, leading to an increase in the product yield. When a wavelength longer than 590 nm, in which the absorption of $_{MoS}$HCDs was significantly reduced (Fig. 1e), was incident into the reaction solution, however, the production yield for NBBA decreased to 34% due to insufficient photon energy. This dependency of the product yields on light power density and wavelength is characteristic for typical photocatalysis. Hence, we clearly suggest that $_{MoS}$HCDs photocatalyze the aerobic oxidative coupling of BA to produce the corresponding product. We additionally calculated the apparent quantum efficiency of $_{MoS}$HCDs for the photocatalyzed transformation of benzylamine to the corresponding product at 410 nm, which was 0.95% (experimental details in SI).

The aerobic oxidative coupling reactions of various amines photocatalyzed by $_{MoS}$HCDs were investigated (Table 1). BAs bearing electron donating groups were converted into the corresponding products at high yields (entries 1-4). However, the product yields of BAs with electron withdrawing groups slightly decreased (entries 5-8). Heterocyclic amino compounds such as pyridine-2-ylmethanamine and thiophene-methylamine were also examined (entry 9-10); they were converted into the corresponding products with slightly lower yields than for BA derivatives. The 1-phenylethylamine (entry 11) was not an active substrate in $_{MoS}$HCDs-photocatalyzed oxidative coupling reaction due to steric hindrance. Secondary dibenzylamine also highly yielded the corresponding imine (entry 12). In addition, an oxidative cross-coupling reaction between BA and heptylamine produced a moderate yield of product (entry 13). These results show that $_{MoS}$HCDs are promising photocatalysts to effectively promote the oxidative coupling reactions of various amines.

Conclusion

In conclusion, we developed a unique hollow interior of photocatalyst $_{MoS}$HCDs doped with a large portion of pyridinic N atoms and MoS_x, which showed outstanding photocatalytic activity in the aerobic oxidative couplings of various amines under visible light irradiation at room temperature. Mechanistic investigations revealed that modulating the type of doping at atomic level and nanostructure was crucial for the significantly enhanced photocatalytic activity of $_{MoS}$HCDs in visible light-driven catalysis. We expect that this chemical approach for a control over doping and nanostructures will be extended to designing effective photocatalysts for diverse photocatalytic reactions.

Acknowledgements

This work was supported by the Basic Science Research Program (NRF-2014R1A2A1A11051877 and 2008-0061891) of the National Research Foundation of Korea (NRF), funded by the Ministry of Science, ICT and Future Planning. It was also supported by the Human Resources Development program (No.20154030200680) of the Korea Institute of Energy Technology Evaluation and Planning (KETEP), through a grant funded by the Korea government Ministry of Trade, Industry and Energy.

Conflict of Interest

The authors declare no competing financial interest.

References

1. S. Y. Lim, W. Shen and Z. Q. Gao, *Chem Soc Rev*, 2015, **44**, 362-381.
2. X. T. Zheng, A. Ananthanarayanan, K. Q. Luo and P. Chen, *Small*, 2015, **11**, 1620-1636.
3. J. H. Shen, Y. H. Zhu, X. L. Yang and C. Z. Li, *Chem Commun*, 2012, **48**, 3686-3699.
4. Y. Q. Dong, H. C. Pang, H. B. Yang, C. X. Guo, J. W. Shao, Y. W. Chi, C. M. Li and T. Yu, *Angew Chem Int Ed*, 2013, **52**, 7800-7804.
5. K. Jiang, S. Sun, L. Zhang, Y. Lu, A. G. Wu, C. Z. Cai and H. W. Lin, *Angew Chem Int Ed*, 2015, **54**, 5360-5363.
6. Y. P. Sun, B. Zhou, Y. Lin, W. Wang, K. A. S. Fernando, P. Pathak, M. J. Meziani, B. A. Harruff, X. Wang, H. F. Wang, P. J. G. Luo, H. Yang, M. E. Kose, B. L. Chen, L. M. Veca and S. Y. Xie, *J Am Chem Soc*, 2006, **128**, 7756-7757.
7. Y. P. Sun, X. Wang, F. S. Lu, L. Cao, M. J. Meziani, P. J. G. Luo, L. R. Gu and L. M. Veca, *J Phys Chem C*, 2008, **112**, 18295-18298.
8. F. Li, C. J. Liu, J. Yang, Z. Wang, W. G. Liu and F. Tian, *RSC Adv*, 2014, **4**, 3201-3205.
9. S. Khan, A. Gupta, N. C. Verma and C. K. Nandi, *Nano Lett*, 2015, **15**, 8300-8305.
10. S. L. Hu, R. X. Tian, Y. G. Dong, J. L. Yang, J. Liu and Q. Chang, *Nanoscale*, 2013, **5**, 11665-11671.
11. H. T. Li, R. H. Liu, S. Y. Lian, Y. Liu, H. Huang and Z. H. Kang, *Nanoscale*, 2013, **5**, 3289-3297.
12. M. Favaro, L. Ferrighi, G. Fazio, L. Colazzo, C. Di Valentin, C. Durante, F. Sedona, A. Gennaro, S. Agnoli and G. Granozzi, *ACS Catal*, 2015, **5**, 129-144.
13. S. I. Murahashi, *Angewan Chem Int Ed Eng*, 1995, **34**, 2443-2465.
14. M. Largeron, *Eur J Org Chem*, 2013, **2013**, 5225-5235.
15. F. Raza, J. H. Park, H.-R. Lee, H.-I. Kim, S.-J. Jeon and J.-H. Kim, *ACS Catal*, 2016, **6**, 2754-2759.
16. S. Sarina, H. Zhu, E. Jaatinen, Q. Xiao, H. Liu, J. Jia, C. Chen and J. Zhao, *J Am Chem Soc*, 2013, **135**, 5793-5801.
17. F. Su, S. C. Mathew, L. Möhlmann, M. Antonietti, X. Wang and S. Blechert, *Angewan Chem Int Ed*, 2011, **50**, 657-660.
18. N. Kang, J. H. Park, K. C. Ko, J. Chun, E. Kim, H.-W. Shin, S. M. Lee, H. J. Kim, T. K. Ahn, J. Y. Lee and S. U. Son, *Angew Chem Int Ed*, 2013, **52**, 6228-6232.
19. X.-J. Yang, B. Chen, X.-B. Li, L.-Q. Zheng, L.-Z. Wu and C.-H. Tung, *Chem Commun*, 2014, **50**, 6664-6667.
20. H. T. Li, Z. H. Kang, Y. Liu and S. T. Lee, *J Mater Chem*, 2012, **22**, 24230-24253.
21. K. A. S. Fernando, S. Sahu, Y. Liu, W. K. Lewis, E. A. Guliants, A. Jafariyan, P. Wang, C. E. Bunker and Y.-P. Sun, *ACS Appl Mater Inter*, 2015, **7**, 8363-8376.
22. S. Young Park, H. Uk Lee, Y.-C. Lee, S. Choi, D. Hyun Cho, H. Sik Kim, S. Bang, S. Seo, S. Chang Lee, J. Won, B.-C. Son, M. Yang and J. Lee, *Sci Rep-Uk*, 2015, **5**, 12420.
23. Q. S. Gao, C. Giordano and M. Antonietti, *Angew Chem Int Ed*, 2012, **51**, 11740-11744.
24. H. A. Benesi and J. H. Hildebrand, *J Am Chem Soc*, 1949, **71**, 2703-2707.
25. L. H. Liu, S. Y. Zhang, X. F. Fu and C. H. Yan, *Chem Commun*, 2011, **47**, 10148-10150.
26. J. N. Coleman, M. Lotya, A. O'Neill, S. D. Bergin, P. J. King, U. Khan, K. Young, A. Gaucher, S. De, R. J. Smith *et al*, *Science*, 2011, **331**, 568-571.
27. S. Mayavan, J.-B. Sim and S.-M. Choi, *J Mater Chem*, 2012, **22**, 6953-6958.
28. L. R. L. Ting, Y. Deng, L. Ma, Y.-J. Zhang, A. A. Peterson and B. S. Yeo, *ACS Catal*, 2016, **6**, 861-867.
29. C. Guimon, A. Gervasini and A. Auroux, *J Phys Chem B*, 2001, **105**, 10316-10325.
30. C. Berrueco, P. Alvarez, S. Venditti, T. J. Morgan, A. A. Herod, M. Millan and R. Kandiyoti, *Energ Fuel*, 2009, **23**, 3008-3015.
31. L. Poulain, A. Monod and H. Wortham, *J Photochem Photobiol A*, 2007, **187**, 10-23.
32. W. A. Saidi, *J Phys Chem Lett*, 2013, **4**, 4160-4165.
33. X. Lang, H. Ji, C. Chen, W. Ma and J. Zhao, *Angew Chem Int Ed*, 2011, **50**, 3934-3937.
34. F. Z. Su, S. C. Mathew, L. Mohlmann, M. Antonietti, X. C. Wang and S. Blechert, *Angew Chem Int Ed*, 2011, **50**, 657-660.
35. X. Liu, L. Zhang, Z. Cheng and X. Zhu, *Polym Chem*, 2016, **7**, 689-700.
36. C. K. Prier, D. A. Rankic and D. W. C. MacMillan, *Chem Rev*, 2013, **113**, 5322-5363.
37. J. Schneider, P. Du, P. Jarosz, T. Lazarides, X. Wang, W. W. Brennessel and R. Eisenberg, *Inorg Chem*, 2009, **48**, 4306-4316.

View Article Online
DOI: 10.1039/C6TA04278C

Graphical Abstract

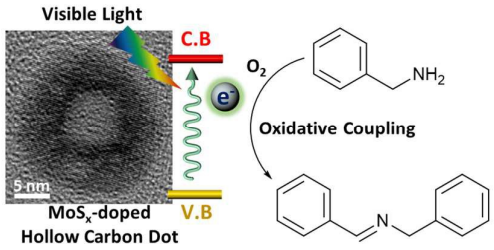

MoS_x-doped hollow carbon dots exhibit outstanding photocatalytic activity in the aerobic oxidative amine coupling reaction at room temperature.